Solvent Effects on the Temperature Dependence of Hydride Kinetic Isotope Effects: Correlation to the Donor-Acceptor Distances

Pratichhya Adhikari, Meimei Song, Mingxuan Bai, Pratap Rijal, Nicholas DeGroot, Yun Lu*

Department of Chemistry, Southern Illinois University Edwardsville, Edwardsville, Illinois 62026, United States

Supporting Information Placeholder

ABSTRACT: Protein structural effects on the temperature (T) dependence of kinetic isotope effects (KIEs) in H-tunneling reactions have recently been used to discuss about the role of enzyme thermal motions in catalysis. Frequently observed nearly T-independent KIEs in the wild-type enzymes and T-dependent KIEs in variants suggest that H-tunneling in the former is assisted by the naturally evolved protein constructive vibrations that help sample short donor-acceptor distances (DADs) needed. This explanation that correlates T-dependence of KIEs with DAD sampling has been highly debated as simulations following other H-tunneling models sometimes gave alternative explanations. In this paper, solvent effects on the T-dependence of KIEs of two hydride tunneling reactions of NADH/NAD^+ analogues (represented by $\Delta E_a = E_{aD} - E_{aH}$) were determined in attempts to replicate the observations in enzymes and test the protein vibration assisted DAD sampling concept. Effects of selected aprotic solvents on the DAD_{PRC}'s of the productive reactant complexes (PRCs) and the DAD_{TRS}'s of the activated tunneling ready states (TRSs) were obtained through computations and analyses of the kinetic data including 2° KIEs, respectively. A weaker T-dependence of KIEs (*i.e.*, smaller ΔE_a) was found in a more polar aprotic solvent in which the system has a shorter average DAD_{PRC} and DAD_{TRS}. Further results show that a charge-transfer (CT) complexation made of stronger donor/acceptor gives rise to a smaller ΔE_a. Overall, the shorter and less broadly distributed DADs resulted from the stronger CT complexation vibrations give rise to a smaller ΔE_a. Our results appear to support the explanation that links the T-dependence of KIEs to the donor-acceptor rigidity in enzymes.

▪ INTRODUCTION

Kinetic isotope effect (KIE) is an important tool to study enzymatic reaction mechanisms and develop theories for enzyme catalysis.[1-8] KIEs on H-transfer processes that are outside of the semiclassical limits have been used to suggest a H-tunneling mechanism that accompanies lower activation energy than the assumed classical pathway. The semiclassical limits include such as small H/D KIE values of 2 – 7 and isotopic activation energy difference ΔE_a (= $E_{aD} - E_{aH}$) of 1.0 – 1.2 kcal/mol.[9] The observed nonclassical KIE behaviors have brought discussions about the chemical and physical roles of enzymes in catalysis. Recent observed unusual temperature (T) dependence of KIEs in enzymes versus their variants has been used to provide insight into the argument as to whether enzyme's local fast dynamics has a role in chemical catalysis.[5,10-13]

Over the past 20+ years, it has been frequently observed that both small and large KIEs on H-transfers are T-independent or weakly T-dependent in wild-type enzymes ($\Delta E_a \sim 0$), but they become T-dependent to various extents in their variants ($\Delta E_a >$ or $>> 0$).[8,14-25] While the traditional Bell tunneling model that assumes a static energy barrier failed to explain the observed trends in ΔE_a's, the vibration-assisted activated H-tunneling (VA-AHT) models, also called the Marcus-like models or environmentally coupled tunneling, built on the basis of the work of Kuznetsov–Ulstrup, as well as the nonadiabatic vibronic H-tunneling treatment, were used to reconcile the results.[5,7,13,18,19,22,26,27] In these treatments, there are two thermal activation processes, one in which heavy atom motions bring the H-donor and acceptor to the tunneling ready states (TRSs) where the activated reactant and product are degenerate for H-tunneling to occur, and the other in which heavy atom motions sample the appropriate donor-acceptor distances (DADs) at the TRS. Since the tunneling DAD is sensitive to the mass of the transferring isotope (H/D/T), only the DAD sampling activation is primary isotope sensitive thus determining the T-dependence of KIEs. Within this model, the weak T-dependence of KIEs is explained in terms of the well-organized reaction coordinate in which the average DAD is short and the range of DADs sampled is narrow, implicating that the wild-type enzyme active site has strong compressive vibrations that press the two reactants close to each other leading to a small isotopic DAD sampling energy difference, *i.e.*, a small ΔE_a. In variants, however, the naturally evolved vibrations are impaired, the average DAD becomes longer, the DAD sampling range becomes broader, therefore, isotopic DAD sampling energy difference becomes large leading to a large ΔE_a. These explanations have been used to support the recently proposed but debated physical origin of enzyme catalysis, which is, constructive local fast thermal motions in enzymes are coupled to the reaction coordinate.

Computational simulations of the T-dependence of KIEs following various contemporary activated H-tunneling models/treatments were carried out to support or disprove the proposed role of enzyme motions in short DAD sampling for catalysis. Quantum mechanical (QM) calculations, together with the molecular mechanical (MM) or molecular dynamical (MD) calculations, were done following the VA-AHT model,[5,28] the nonadiabatic vibronic model,[23,29,30] the ensemble averaged variational TS theory with multi-dimensional H-tunneling (EA-VTST/MT),[31-33] as well as the empirical valence bond theory[10,34,35]. The VA-AHT model was used to explain the observations including those for hydride/proton transfer reactions,[13,36] whereas the vibronic model was mainly for the nonadiabatic H-atom transfer reactions[6]. While both contain the activated DAD sampling

concept in the ground state tunneling mechanism at the TRS,[13,19,27,29,37] some researchers argued that the VA-AHT model should not be used to explain the adiabatic hydride/proton tunneling that likely involves the excited state of product at the TRS.[38] Other researchers, however, have attempted to extend the VA-AHT model to fit their results for the adiabatic hydride or proton transfer reactions.[7,13,21,24,27,39-41] On the other hand, theoretical replications of the observed huge KIEs for the H-atom transfer reactions in lipoxygenases using the EA-VTST/MT appeared to have encountered difficulty.[11,31,37,42] Nevertheless, even simulations using the latter model and the empirical valence bond theory for some enzyme catalyzed hydride/proton transfer reactions show that the weak T-dependence of the KIEs results from the insensitivity of the DAD's to temperature, seemingly supporting the compressive dynamics in the active site of the enzymes.[8,10,27,29,32,43] Other studies have, however, shown that they could also result from the effects of temperature on the microscopic mechanism, for example, on the position of the TS and the shape of the potential barrier.[10,31] In another study, the QM/MM/MD simulations ascribed the different ΔE_a's to the higher entropic barrier in the variant than in the wild-type enzyme.[44] Use of the T-dependence of KIEs to implicate the DAD sampling catalysis has been highly debated.

We regard that the ideas about the correlation of T-dependence of KIEs with DAD sampling activation in enzymes could be tested by study of the "simpler" reactions in solution, for which DADs could be controlled by structural or solvent effects. Our purpose is thus to design H-transfer reactions in solution in attempt to study this correlation, if any. We have proposed a hypothesis on the basis of the above explanations for enzymes. The hypothesis is that the more rigid the reaction system, the more difficult for the DAD to change with temperature, the weaker the T-dependence of KIEs will be.[45-47] Here, a rigid TRS can be a tightly associated one with strong electronic attractions between donor and acceptor, and/or with steric factors that minimize the flexibility of the two reaction centers, and/or with strong solvation effects that stabilize the TRS and thus strengthen the donor-acceptor attraction in it. Investigation of the hypothesis is expected to provide insight into the role of protein motions in catalysis and opens a new research direction that studies the relationship between structure and T-dependency of KIEs for general H-transfer reactions.

We have reported the structural effects on the T-dependence of KIEs of several hydride transfer reactions of NADH/NAD^+ analogues in solution.[45-48] We found that a smaller ΔE_a accompanies with more reactive donor/acceptor that form stronger charge-transfer (CT) complexations.[45,46] We also found that in some of the systems the more crowded reaction centers did appear to correspond with a smaller ΔE_a.[45,46] These results support our hypothesis. In those studies, the short tunneling DADs would be mainly sampled by the CT complexation thermal vibrations.

In this paper, we attempt to use solvent effects to mediate the stability or vibrational rigidity of the CT complexation of the same class of hydride transfer systems to further investigate our hypothesis. Since the corresponding activated reaction complex involves a dispersed positive charge, its CT complex is expected to be stabilized and thus more rigid in a more polar solvent. Also, the hydride donor has rich π-electron density that could form H-bonding interaction with the hydroxylic solvents so that the CT complexation is expected to be loose. Therefore, study of the effects of protic/aprotic solvents of various polarities on the T-dependence of KIEs of these reactions could serve for this research purpose.

Herein, we chose hydride transfer reactions from diethyl 1,4-dihydro-2,6-dimethyl-3,5-pyridinedicarboxylate (HEH , Hantzsch ester) and 2-phenyl-1,3-dimethyldihydroimidaroline (DMPBIH) to N-methylacridinium ion ($MA^+BF_4^-$) for this solvent effect study (Eqn. (1)). The two hydride donors have very different structures and reactivities, and we have reported the T-dependence of KIEs for both of the reactions in acetonitrile.[45] We will compare these results with those in solvents of various polarities to study the bulk (macroscopic) solvent effects on the T-dependence of KIEs and with those in the hydroxylic protic solvents to study the microscopic solvent effects on the same. Moreover, all possible productive reactant complexes (PRCs) along with their DAD_{PRC}'s in selected aprotic solvents (acetonitrile *vs.* the much less polar solvent of chloroform) were computed. The corresponding DAD_{TRS} information derived from the kinetic data including secondary (2°) KIEs at positions labeled in Eqn. (1) will be compared with the DAD_{PRC}'s to discuss about the solvent polarity effects on the DAD_{TRS}'s sampling from PRCs. Correlation of the DAD information with the observed T-dependence of KIEs will be discussed. Combining the protic solvent effects results, we will show that the polar aprotic solvent does give rise to a shorter average DAD_{PRC}/DAD_{TRS} and a weaker T-dependence of KIEs. On the other hand, we will compare the effects of DMPBIH *vs.* HEH on the T-dependence of KIEs. We will show that a stronger CT complexation with the more reactive DMPBIH gives rise to a weaker T-dependence of KIEs in all of the solvents studied. Both solvent and structural effect studies appear to support our hypothesis that links system rigidity to the T-dependence of KIEs. Our results could provide information to the understanding of the relevant enzymatic reactions and for the development of potential future theories for hydride- as well as general H-transfer reactions.

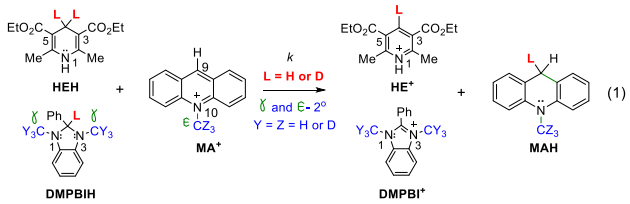

Special abbreviations frequently used in this paper are listed here for the readers to quickly catch their meanings. They include: TRS (tunneling ready state), DAD (donor-accept distance), CT (charge-transfer), and PRC (productive reactant complex).

▪ EXPERIMENTAL

The syntheses of HEH, and HEH-4,4'-d,d, DMPBIH, DMPBIH-2-d, 1,3-N,N-$2CD_3$ substituted DMPBIH, MA^+ (counter ion: BF_4^-) and 10-CD_3 substituted MA^+, can be found from our recent publications.[45,46] The HPLC grade acetonitrile solvent was redistilled twice, over $KMnO_4/K_2CO_3$ to remove the reducing impurities and P_2O_5 to remove water, in order, under nitrogen. The isobutyronitrile was redistilled over P_2O_5 under nitrogen. The HPLC grade chloroform was refluxed over molecular sieves and redistilled under nitrogen. Isopropanol was redistilled and absolute ethanol was used as purchased. Isopropanol and ethanol were purged with nitrogen before use for kinetic measurements. Kinetic solutions were prepared using the freshly distilled solvents and kept in the refrigerator (4 °C) or freezer (-20 °C) before use at each kinetic temperature conditions.

Kinetics were determined on the SF-61DX2 Hi-Tech KinetAsyst double-mixing stopped-flow instrument. Same kinetic procedures in our publications were followed.[45,46,49] From our experiments and literature, the type of reactions strictly follow the second-order rate law.[45,46,48-52] Each KIE was derived from the second-order rate constants of the isotopic reactions (= k_{2H}/k_{2D}). Experimentally, the pseudo-first order rate constants (k^{pfo}'s) were determined

spectroscopically (by UV-Vis) and the observed k_2 was calculated from dividing k^{pfo} by the concentration of the large excess reactant (for example, R-H or R-D), *i.e.*, $k_2 = k^{pfo}/[R\text{-}H(D)]$. Then,

$$KIE = \frac{k_{2H}}{k_{2D}} = \frac{k_H^{pfo}}{k_D^{pfo}} \times \frac{[R-D]}{[R-H]} \qquad (2)$$

Usually, the same concentrations of R-H and R-D solutions were used, but in order to eliminate the errors in the preparation of the two solutions of certain concentration, we corrected the concentration ratio by measuring the absorbance (*Abs*) of each isotopic solution at an appropriate wavelength. (This is especially necessary for the measurements of small 2° KIEs.) Assuming R-H and R-D have the same extinction coefficient at the wavelength ($\varepsilon_H = \varepsilon_D$), we have

$$KIE = \frac{k_{2H}}{k_{2D}} = \frac{k_H^{pfo}}{k_D^{pfo}} \times \frac{Abs_D}{Abs_H} \qquad (3)$$

For the 2º KIE comparison in between acetonitrile and chloroform, we determined the $\varepsilon_H/\varepsilon_D$ on DMPBIH in the respective solvents and found it is close to unity within the experimental error. Note that the Abs_H and Abs_D were usually found very close. We ascribe the closeness between the two largely to the use of the high precision Mettler Toledo™ XSR analytical balance (0.01 mg) for kinetic solution preparation in our lab.

Six measurements of k^{pfo}'s for the reactions of two isotopologues for 1° and 2° KIE derivations at different temperatures were made on the same day and repeated on, at least, two other days. For a ΔE_a determination, kinetics was determined over a temperature range of 40 °C, and the E_{aH} and E_{aD} were derived, respectively. A typical kinetic procedure at certain temperature is as follows. Six kinetic runs of 12 half-lives of the reaction were measured for each isotopic reaction back to back. The procedure was then repeated at other temperatures as quickly as possible (5, 15, 25, 35, 45 °C, in order) so that the instrument settings were kept the same and the aging of the reaction solutions was the minimum (the solutions were wrapped with aluminum foil and kept in refrigerator between temperatures. The same procedure was used with a freezer of -20 °C and the same results were obtained). Repetitions on different days sometimes used different batches of substrates and solvents and sometimes were done by different workers. That was to eliminate the effect of possible different impurity from unknown sources or human errors on the KIE measurements. Therefore, one KIE value was obtained from *at least* 18 repetitions. For the measurements of the small 2º KIEs, sometimes more than 18 repetitions were made to ensure the difference that we found is meaningful (see Tables S12 and S13). Pooled standard deviations were reported. All of the kinetic results (from the extent of reaction of 1% to 99.98% (corresponding to 12 half-lives)) were fitted very well/excellently to the first-order rate law for k^{pfo} derivation and to the Arrhenius correlations for E_a derivation, both with $R^2 = 0.9990 – 1.0000$, mostly closer or sometimes even equal to 1.0000! Other details about the kinetic measurements can be found from Tables S1 to S13.

▪ COMPUTATIONS

Gaussian 09 and the universal continuum solvation (SMD) model[53] were used for all of the computations.

PRC Computations

All structures were optimized using the M06-2X density functional.[54] Initial geometries of the TS's and reactant complexes were first optimized in gas-phase with the Def2-SVP basis set.[55] The productive reactant complexes (PRC's) were confirmed by the intrinsic reaction coordinate analysis. These structures were further refined in acetonitrile and chloroform by using the Def2-TZVP basis set[55] with the ultrafine DFT integration grid and the SMD solvation model. The latter settings of computations were used to calculate the thermal corrections to the Gibbs free energies (E_{G_corr}) and the single point energies (E_{sp}) of these geometries. Free energies (G's) of the optimized structures are the sum of E_{G_corr} and E_{sp}. Due to the overestimate nature of the harmonic model, further treatments were needed to correct them to derive the E_{G_corr}. A frequency scaling factor of 0.9708 was fitted against the ZPVE15/10 database[56] for the purpose. Detailed procedure for calculating the scaling factor can be found from the method in literature.[56]

The abundance (A_i) of each optimized conformation (i) for each reaction system was calculated according to the Boltzmann distribution of its energy (G_i) over the sum of such Boltzmann distributions of all PRC conformations,

$$A_i = (e^{-\frac{G_i}{kT}}) / \sum_1^N e^{-\frac{G_i}{kT}} \qquad (4)$$

where N is the number of conformations, k is the Boltzmann constant, T is temperature.

The weighted average DAD_{PRC} was calculated by summing up the fractional DADs of all of the PRC conformations, each of which was obtained by multiplying the individual DAD_i with the corresponding abundance (A_i). The formula to calculate the weighted average DAD_{PRC} is as follows,

$$Weighted\ average\ DAD_{PRC} = \sum_1^N \mathrm{DAD_i}\, A_i \qquad (5)$$

2º KIE and 2º Equilibrium Isotope Effect (EIE) Computations

The calculations were performed under the M06-2X[87]/Def2-SVP[88] level of theory with ultrafine DFT integration grid. A fitted frequency scaling factor of 0.9695 is used to minimize the overestimation error of the harmonic model.

The ground-state reactants and products as well as the classical TS structures were optimized. The free energies of these structures and their isotopologues were calculated to derive the classical 2° KIEs and the 2° EIEs. Detailed procedures can be found in the *Supporting Information (SI)*.

▪ RESULTS

It is well known that hydride-transfer of the NADH/NAD$^+$ model reactions takes place within a CT complex of reactants.[45,57-59] In this paper, we call these complexes PRCs. We have reported the spectroscopy evidence for the CT complex formation for the two reactions in acetonitrile.[45] The PRCs are believed to form in a diffusion-controlled rate. Meanwhile, there could be nonproductive reaction complexes (RCs) in fast equilibrium with the free reactants and PRCs. Theoretically, the hydride-transfer could be classical through a transition state (TS) or nonclassical through a TRS. This mechanism is described in Eqn. (6) (Don-H and Acc refer to donor

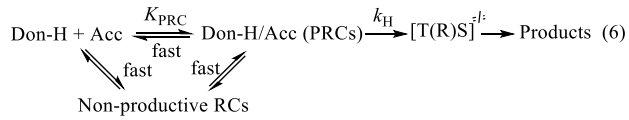

and acceptor, respectively). The observed KIEs are derived from the observed k_2's. They correspond with the hydride transfer step (k_H). That is, $KIE = k_{2H}/k_{2D} = k_H/k_D$.

The k_2's and KIEs at temperatures from 5 to 45 °C were carefully determined and they have relatively small standard deviations (also see Experimental and *SI*). The representative $k_2^{25°C}$'s as well as the

ΔE_a's derived are listed in Table 1. Note that the α-2° KIE on HEH should be contained in the observed KIEs, but since the 2° KIE is usually small,[49,60,61] its T-dependence is expected not to significantly affect the ΔE_a.[45,48] The dielectric constant (ε_r) for the single solvent as well as the estimated ε_r's for the mixed solvents are listed in the Table as well. For the latter, the ε_r was calculated using the formula $\varepsilon_r = (V_1/V)\bullet\varepsilon_r(1) + (V_2/V)\bullet\varepsilon_r(2)$, where $V_{1(2)}/V$ is the volume percentage of the two single solvents in the mixed solvents. For the reactions in the hydroxylic solvents, we added 5.0 x 10^{-5} M HBF_4 to prevent MA^+ from forming the corresponding alcohol/water adducts.[52,62] For the study of the hydroxylic solvent effects, we compare the results with those from the reactions in acetonitrile. The dielectric constants of these solvents are similar so that the discussion of the expected microscopic solvent effects would be meaningful. Figure 1 shows the exemplified Arrhenius plots of KIEs in selected aprotic solvents. The same in the hydroxylic solvents are given in the *SI* (Figure S1). In general, ΔE_a increases with decreasing solvent polarity and slightly increases with changing from acetonitrile to protic solvents. Moreover, ΔE_a is greater for the reaction of HEH than the reaction of DMPBIH in both solvents.

Unusual KIE behaviors to suggest an H-tunneling mechanism

The first impression of the data in Table 1 is that all of the KIEs are smaller than 7 being classical. For the reaction of HEH, the ΔE_a's are from 0.95 – 1.26 kcal/mol being within the semiclassical range of 1.0 – 1.2 kcal/mol ; for the reaction of DMPBIH, however, they are from 0.43 – 0.70 kcal/mol, being well outside of the classical range. At least the observed nonclassical ΔE_a's for the latter reaction are not compatible with the "classical" small KIE values, suggesting nonclassical H-tunneling mechanisms. While such hydride transfer reactions of NADH/NAD^+ analogues usually have small KIEs, both this and other works of ours as well as a few

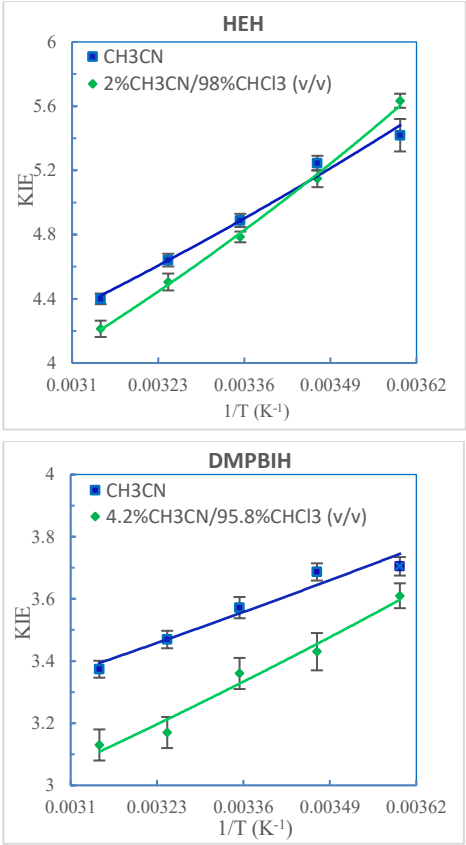

Figure 1. Arrhenius plots of the KIEs for the reactions of HEH and DMPBIH with MA^+ in selected aprotic solvents (from 5 to 45 °C). Lines represent the nonlinear regressions to an exponential equation.

Table 1. Reaction rates and T-dependence of KIEs in different solvents

	Solvents	ε_r [a]	$k_{2H}^{25°C}$ ($M^{-1}s^{-1}$) [b]	1° KIE range [c]	ΔE_a (kcal/mol) [b]
			Reaction of HEH with MA^+		
	Aprotic Solvents				
1 [d]	Acetonitrile	37.5	1.57(0.01) x 10^2	5.42 – 4.40	0.95 (0.10)
2	Isobutyronitrile	21.0	1.99(0.01) x 10^2	5.70 – 4.24	1.27 (0.12)
	Chloroform/Acetonitrile (v/v)				
3	50%/50%	~21.2	1.54(0.01) x 10^2	5.73 – 4.40	1.13 (0.05)
4	80%/20%	~11.3	3.25(0.03) x 10^2	4.82 (0.05) [b,e]	n.d. [f]
5	90%/10%	~8.1	1.40(0.01) x 10^3	4.92 (0.03) [b,e]	n.d. [f]
6	95%/5%	~6.4	4.20(0.03) x 10^3	4.75 (0.11) [b,e]	n.d. [f]
7	98%/2%	~5.5	9.28(0.05) x 10^3	5.63 – 4.21	1.26 (0.05)
	Hydroxylic Solvents				
8 [g]	Isopropanol/water	~30.3	2.80(0.01) x 10^2	5.92 – 4.59	1.11 (0.07)
9 [g]	Ethanol/water	~35.6	2.84(0.02) x 10^2	5.90 – 4.54	1.13 (0.05)
			Reaction of DMPBIH with MA^+		
	Aprotic Solvents				
10 [h]	Acetonitrile	37.5	2.12(0.02) x 10^2	3.70 – 3.37	0.43 (0.15)
11	Isobutyronitrile	21.0	1.90(0.01) x 10^2	3.65 – 3.10	0.70 (0.27)
	Chloroform/Acetonitrile (v/v)				
12	95.8%/4.2%	~6.2	3.44(0.02) x 10^2	3.61 – 3.13	0.64 (0.08)
	Hydroxylic Solvents				
13 [g]	Isopropanol/water	~30.3	2.82(0.02) x 10^2	3.75 – 3.28	0.59 (0.10)

[a] Dielectric constant, see texts; [b] Numbers in parentheses are standard deviations (see *SI* for the raw data); [c] From 5 to 45 °C, unless otherwise noted; [d] From Table 1 of ref.[45], repeated and combined with the data from this work; [e] At 25 °C only; [f] Not determined; [g] 80% alcohol/20% water (v/v), containing 5.0 x 10^{-5} M HBF_4; [h] From Table 1 of ref.[45].

sporadic work from others showed that they have ΔE_a's spanning a wide range from well below the semiclassical limit, through the semiclassical range, to well above the semiclassical limit (up to ~ 1.8 kcal/mol).[45,46,48,63,64] Furthermore, it has been shown that small KIEs from such hydride transfer reactions also fit to the Marcus theory of atom transfer that involves a H-tunneling component.[52,65,66] In the meantime, the small KIE's and similar ΔE_a's were also found in the hydride transfer reactions of NADH/NAD$^+$ in enzymes and variants.[8,13,21,27,39,67] As described in the Introduction, the latter observations have been explained following various activated H-tunneling models.

On the other hand, the frequently observed unusual 2° KIEs outside of their semiclassical limits in these and similar hydride transfer reactions in both solution (our work[49,68,69]) and enzymes[1,5,70-76] have also been used to demonstrate a H-tunneling mechanism. In this work, the 1,3-γ,γ-2CH_3/2CD_3 2° KIEs on DMPBIH and 10-ε-CH_3/CD_3 2° KIEs on MA$^+$ for their reactions in acetonitrile and chloroform were determined and are listed in the subsequent Table 3. While the γ-2° KIEs on DMPBIH are close to the computed classical ones (Table 3), the ε-2° KIEs on MA$^+$ deviate from them significantly. Also, we have reported the ε-2° KIEs on MA$^+$ (1.01) for its reaction with HEH in acetonitrile.[49] The computed classical one in this work is, however, 1.11 (Table 3 footnote c), further suggesting that the reaction goes by a nonclassical mechanism.

Therefore, use of Bell's semiclassical limits of (1°) KIEs to evaluate whether the class of hydride transfer reactions uses a H-tunneling mechanism appears to be not proper.[77] The question in this paper research is whether the ΔE_a is linked to the DAD_{TRS} sampling activation process that has been described in the VA-AHT model and the nonadiabatic vibronic H-tunneling model and that has been sometimes implicated or discussed in studies following other activated H-tunneling models.

Selected aprotic solvent effects on DAD_{PRC}'s: Acetonitrile vs. chloroform

For correlation of the ΔE_a to the DAD sampling process from PRCs to TRSs, information about the respective DAD's would be needed. In literature, the DAD_{PRC}'s and DAD_{TRS}'s have been obtained for the correlation study. For example, the DAD_{PRC} information was achieved by studying the stable reactant (Michaelis) complex structure in enzymes (with an inhibitor or modification of the cofactor) using the NMR technique[27,67,78] as well as the QM and MD calculations[8,45,79]. We have used QM-DFT method to compute the DAD_{PRC} information for several hydride transfer systems of NADH/NAD$^+$ analogues in acetonitrile (using the SMD model) and found that, like in enzymes, the shorter average DAD_{PRC} corresponds with a smaller ΔE_a.[45] Indeed, that study includes both of the hydride transfer reactions studied in this paper. In that work, 8 and 3 PRCs were found for the reactions of HEH(Me) and DMPBIH with MA$^+$ in acetonitrile, respectively. (We used the dimethyl ester groups (HEH(Me)) to replace the diethyl ester groups in the normal HEH for less computing time.)

In this work, 8 and 3 PRCs for the same reactions of HEH(Me) and DMPBIH were optimized in chloroform to compare with the corresponding DAD_{PRC} distributions in acetonitrile.[45] Figure 2 shows the most populated CT complex geometries in each solvent. Table 2 lists the range of the DAD_{PRC}'s, the weighted average DAD_{PRC}'s, as well as the most populated DAD_{PRC}'s, for both systems in the two solvents. Figure 3 shows the direct comparison of the DAD_{PRC} distributions of the two reactions. More than 98% of the PRCs in acetonitrile have DAD_{PRC}'s ranging from 3.39 – 3.49 Å for the reaction of HEH and from 3.31 – 3.55 Å for the reaction of DMPBIH, whereas in chloroform the DAD_{PRC}'s are significantly longer with 3.42 – 3.57 Å for HEH and 3.36 – 3.56 Å for DMPBIH. Importantly, the weighted average DAD_{PRC} was found shorter in acetonitrile than in chloroform for both systems (3.48 Å *vs.* 3.52 Å (for HEH), and 3.39 Å *vs.* 3.50 Å (DMPBIH)), and the DAD_{PRC} for the most populated PRC is also shorter in acetonitrile than in chloroform (3.49 Å *vs.* 3.51 Å (HEH), and 3.31 Å *vs.* 3.56 Å (DMPBIH)). Another information is that the average DAD_{PRC}'s are longer in the reactions of HEH than those in the reactions of DMPBIH in both solvents (3.48 Å (HEH) *vs.* 3.39 Å (DMPBIH) in acetonitrile, and 3.52 Å (HEH) *vs.* 3.50 Å (DMPBIH) in chloroform).

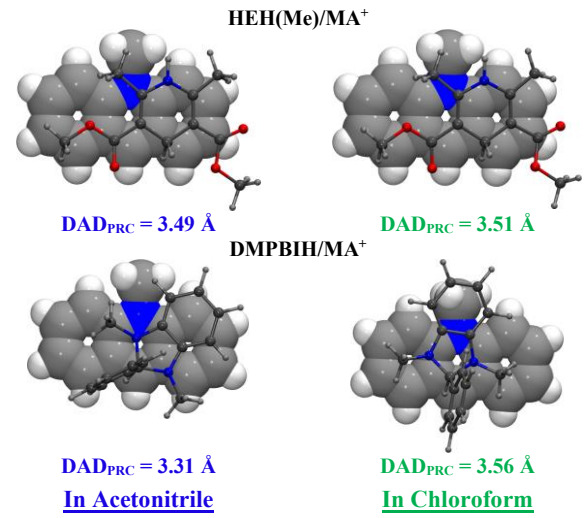

Figure 2. Geometries of the most populated PRCs (with the lowest free energy (G)) of the reactions from HEH(Me) and DMPBIH to MA$^+$ in acetonitrile (ref.[45]) and chloroform (this work) at 25 °C. The space-filling structure in the background represents MA$^+$, the ball-stick structures in the foreground represent different donors. Geometries of all PRCs can be found in the *SI* of ref[45].

Table 2. Comparison of the DAD_{PRC}'s in the PRCs of the reactions in acetonitrile and chloroform [a]

Solvents	DAD_{PRC}'s			
	Range for all Populations	Range for top 98% Populations	Weighted-average [b]	In most populated PRCs [b]
HEH(Me)/MA$^+$ (Total of 8 PRCs found)				
Acetonitrile	3.39 – 3.64	3.39 – 3.49	3.48	3.49
Chloroform	3.42 – 3.59	3.42 – 3.57	3.52	3.51
DMPBIH/MA$^+$ (Total of 3 PRCs found)				
Acetonitrile	3.31 – 3.60	3.31 – 3.55	3.39	3.31
Chloroform	3.36 – 3.62	3.36 – 3.56	3.50	3.56

[a] At 25 C; [b] According to the percent populations of the PRCs.

These results suggest that (1) the PRCs in both systems are statistically more rigid in acetonitrile than in chloroform, and (2) the PRCs in the reactions of DMPBIH are more rigid than those for the reactions of HEH. These are consistent with our expectations that the positively charged PRC would be more stable and tighter in a more polar solvent as well as in a reaction system of stronger electron/hydride donor/acceptor. Note that DMPBIH is 15.2 kcal/mol more reactive than HEH in donating a hydride ion in acetonitrile.[51]

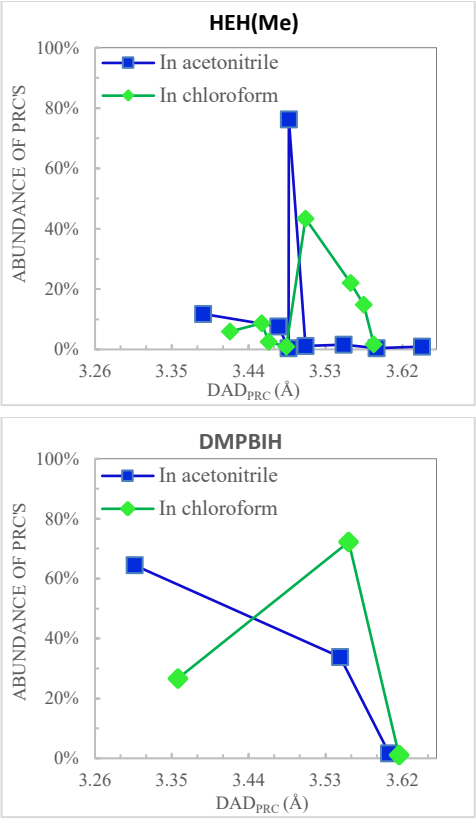

Figure 3. The computed DAD_{PRC} distributions for the hydride transfer reactions from HEH(Me) and DMPBIH to MA^+ in acetonitrile *vs.* chloroform at 25 °C. The same x-axis scale is used for both plots for the purposes of a direct comparison of the two systems.

Selected aprotic solvent effects on DAD_{TRS}'s: Acetonitrile vs. chloroform

The TRS structural information can only be obtained by kinetic studies. In literature, the α-2° KIE has been used as a measure of the TRS rigidity/tightness.[27] We have attempted to use the 1,3-N,N-$2CH_3/2CD_3$ γ-2° KIEs on DMPBIH for its hydride transfer to 9-(*para*-substituted)phenylxanthylium ions to obtain the substituent effect on DAD_{TRS}'s.[46,47] Here in this study, we were able to determine the N-CH_3/CD_3 2° KIEs on both DMPBIH and MA^+ to evaluate the electronic structure and the rigidity order of the TRS's of their reactions in acetonitrile *vs.* chloroform. For the reaction of HEH, however, no such 2° KIE on HEH is available. The effects of acetonitrile/chloroform mixture solvents on kinetics of the latter reaction were then found able to provide the structural information for the TRS's in the two single solvents. Below we will present the solvent effects on the TRS rigidity of the two systems separately.

For the reaction of DMPBIH: The 2° N-CH/CD KIE originates from the decrease/increase in negative hyperconjugation between the lone-pair of electrons on N and σ* orbital of the C-H/D bond due to the loss/gain of electron density on N during the reaction.[45,80] The electron density loss tightens the C-H/D bonds, leading to an inverse 2° KIE, whereas the electron density gain loosens the C-H/D bonds, leading to a normal 2° KIE.[80,81] According to this analysis, the 1,3-N,N-$2CH_3/2CD_3$ γ-2° KIEs on DMPBIH should be inverse while the 10-N-CH_3/CD_3 ε-2° KIEs on MA^+ be normal. Since the more loss of electrons from DMPBIH and/or more gain of electrons to MA could implicate a stronger CT-complexation, a more inverse γ-2° KIE on DMPBIH or a more normal ε-2° KIE on MA^+ are expected to correspond with a tighter TRS complex.

Table 3 lists the observed N-CH_3/CD_3 2° KIEs on both DMPBIH (6H *vs.* 6D) and MA^+ (3H *vs.* 3D) in acetonitrile and chloroform (containing 4.2% (v/v) acetonitrile), respectively. The observed inverse γ-2° KIEs on DMPBIH and normal ε-2° KIEs on MA^+ are consistent with our expectations. The results show that the γ-2° KIE on DMPBIH is more inverse in acetonitrile (0.88) than in chloroform (0.92), but the ε-2° KIE on MA^+ appears to change insignificantly with the two solvents (1.03). While the apparently different γ-2° KIEs suggest that the positive charge density on the DMPBIH moiety of the TRS is more in acetonitrile than in chloroform, the observed same ε-2° KIEs suggest that the positive charge densities at the MA moiety are the same or experimentally indistinguishable for the two solvent systems (due to the smaller number of H/D's as well as the smaller magnitude). Nonetheless, at least the different γ-2° KIEs on DMPBIH suggest that the TRS is a tighter CT complex and has a shorter DAD_{TRS} in acetonitrile than in chloroform.

Table 3. The observed *vs.* computed N-CH_3/CD_3 2° KIEs/EIEs for the reaction of DMPBIH with MA^+ at 25 °C

	γ-$2CH_3/2CD_3$ on DMPBIH	ε-CH_3/CD_3 on MA^+
	Observed 2° KIEs [a]	
Solvents		
Acetonitrile	0.88 (0.01) [b]	1.03 (0.01)
95.8%Chloroform/4.2%acetonitrile (v/v)	0.92 (0.01)	1.03 (0.01)
	Computed 2° EIEs [c,d]	
Acetonitrile	0.74	1.21
Chloroform	0.71	1.26
	Computed classical 2° KIEs [c]	
Acetonitrile	0.88	1.07
Chloroform	0.93	1.13

[a] Data in paratheses are standard deviations (see raw data in Tables S12 and S13); [b] Same as the one we reported previously[49], see Table S12; [c] Using the SMD solvation model (slightly different from the previously computed (with acetonitrile only) using the polarizable continuum solvation model[49]). Classical 2° KIE of 1.11 on MA^+ was also computed for its reaction with HEH in acetonitrile (see earlier text); [d] For DMPBIH to release or for MA^+ to accept a hydride ion.

Estimation of the charge (ξ) distribution in the π-moieties of the TRS could further help evaluate the system tightness. This can be done by comparing the N-CH_3/CD_3 2° KIEs with the corresponding equilibrium isotope effects (EIEs) that reflect a full (+) charge change from reactant to product. The 2° EIEs in acetonitrile and chloroform were computed and are listed in Table 3 as well. Using ξ = (1-KIE)/(1-EIE) for the DMPMIH moiety and ξ = 1 - (KIE-1)/(EIE-1) for MA,[49] it was found that the DMPBIH carries 0.46+ charge and the MA carries 0.86+ charge at the TRS in acetonitrile, whereas in chloroform the charges are 0.28+ and 0.88+, respectively. To balance the 1+ total charge of the system, the negative charge borne by the in-flight nucleus together with that for the CT bonding can be calculated, which are 0.32- in acetonitrile and 0.16- in chloroform. The electronic TRS structures in the two solvents may be described as follows:

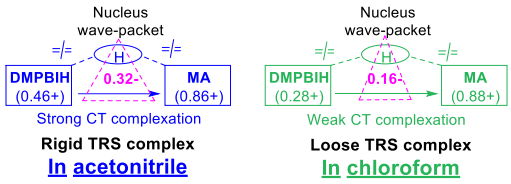

These semi-quantitative results show that the TRS has higher electron density in between the DMPBIH and MA in acetonitrile

than in chloroform, which makes the two moieties more tightly bound to each other in the former solvent.

The corresponding classical γ- and ε-2° KIEs computed are also listed in Table 3 for comparison to the observed ones. As discussed earlier, the overall mismatching between the classical and observed ones together with the observed abnormal ΔE_a values of the system have been used to suggest that the reaction does not take place by a classical mechanism.

For the Reaction of HEH: Table 1 shows that the reaction rate ($k_{2H}^{25°C}$) generally increases with decrease in ε_r of the aprotic solvents. For example, the rate increases by about 1.3-fold when the solvent is changed from acetonitrile to the less polar isobutyronitrile and by 59.0-fold when it is changed to a much less polar chloroform solvent (containing 2% (v/v) acetonitrile). This can be interpreted in terms of more desolvation of the positively charged MA^+ reactant state (RS) by the less polar solvent than that for the TRS in which the (+) charge is dispersed over the two reactant moieties so that the activation energy becomes smaller. Interestingly, for the cases in the mixed solvents of chloroform and acetonitrile, the rate does not increase significantly with adding chloroform to acetonitrile until the mixture becomes about 80%chloroform/20%acetonitrile (v/v) when it starts to increase rapidly (Table 1). This is plotted in Figure 4. The rate change is not proportionally consistent with the change in ε_r. This suggests an unsymmetrical local solvation effect[82] around both the RS (HEH and MA^+) and TRS by the two solvents, with the polar acetonitrile solvation shell being immediately around the RS and TRS and the much less polar chloroform solvation shell outside. When the chloroform content reaches about 80% (v/v), the acetonitrile solvation shell starts to become thin enough to make the desolvation effects by chloroform to function significantly so that the rate starts to increase rapidly. Overall, these analyses suggest that the TRS is less stable and thus easier to break back to reactants in a less polar solvent. Since the stability of a TRS would be largely determined by the strength/tightness of the CT complexation, a less polar solvent would make a weaker/looser CT complexation and likely a longer average DAD_{TRS}. The insets **A** to **D** in Figure 4 represent the local solvation effects on the TRS's and a gradual increase in DAD_{TRS} with adding chloroform. Importantly, the order in DAD_{PRC}'s from acetonitrile to chloroform in this system is consistent with the DAD_{TRS} order.

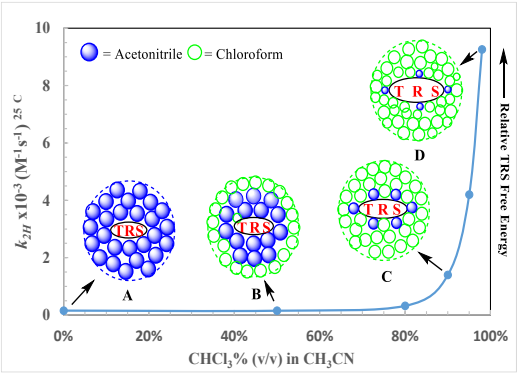

Figure 4. Second-order rate constants of the reaction of HEH with MA^+ as a function of the volume percentage of chloroform in acetonitrile. The insets **A-D** are the schematic description of the unsymmetrical local solvation shells of the TRS for certain mixed solvents. The positively charged TRS is much better solvated by and thus much more rigid in acetonitrile than by/in chloroform. The TRS is loosely associated but the corresponding reaction is faster in chloroform than in acetonitrile (see text).

To summarize, the shorter DAD_{PRC}/DAD_{TRS} in acetonitrile than in chloroform in both systems suggests that a more polar aprotic solvent accompanies with a shorter DAD_{PRC}/DAD_{TRS}. A comparison of the DAD thermal sampling processes from PRCs to TRSs in acetonitrile *vs.* chloroform may be described in Figure 5 (Literature reported that the *dominant* DAD_{TRS} for H-tunneling to occur is ~2.7 Å.[37]). The overall DAD compressive forces for the DAD_{TRS} sampling would come from the "sum" of the constructive CT complexation vibrations from each PRC.

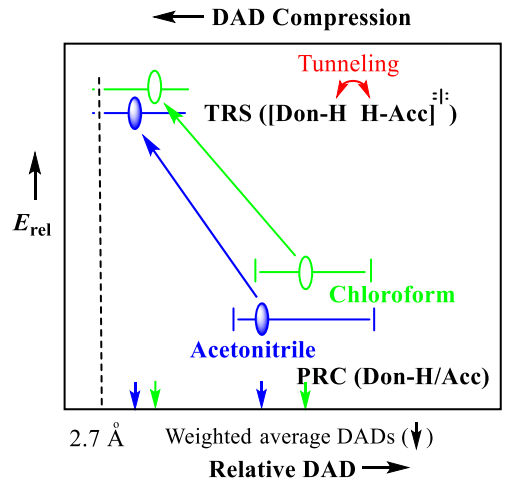

Figure 5. Proposed collective DAD_{TRS} sampling coordinate from different PRCs in acetonitrile *vs.* chloroform (Don-H and Acc refer to donor and acceptor). The solid and open ovals represent the PRCs/TRSs of weighted average DADs from all of the conformations. For each range of the $DAD_{PRC/TRS}$'s, energy of different conformations should not be the same and the PRC/TRS conformations at the "oval" position correspond with the minimum energy state (like a Morse-type curve). For both the PRC and TRS, the average energy is higher in chloroform than in acetonitrile, and the difference would be greater in PRCs than in TRSs as the positive charge is more dispersed in TRSs so that the desolvation by chloroform is less.

▪ DISCUSSION

Table 1 shows that the ΔE_a *generally* increases with decreasing the solvent polarity. For example, from acetonitrile to isobutyronitrile to chloroform (with a small amount of acetonitrile), ΔE_a changes from 0.95 to 1.27 to 1.26 kcal/mol for the reaction of HEH and from 0.43 to 0.70 to 0.64 kcal/mol for the reaction of DMPBIH. Note that the change from isobutyronitrile to chloroform for both reactions seems unexpected in terms of the dielectric constant difference. In this case, some microscopic solvent effect may have played an important role in complicating the trend. Meanwhile, we also noticed that the standard deviations of ΔE_a's for the reactions in isobutyonitrile are relatively large. Nevertheless, a comparison of the DAD_{TRS} sampling information in acetonitrile *vs.* chloroform (Figure 5) with the ΔE_a trend strongly suggests that a more rigid TRS of shorter and narrowly distributed DAD_{TRS}'s corresponds with a smaller ΔE_a. This supports our hypothesis that links the magnitude of ΔE_a with the ease of DAD_{TRS} sampling activation in H-tunneling reactions.

The ΔE_a appears to be slightly larger in the protic solvent than in the aprotic acetonitrile for both reactions. For example, for the solvents from aqueous isopropanol(ethanol)/water to acetonitrile that have the similar dielectric constants, it changes from 1.11(1.13) to 0.95 kcal/mol for the reaction of HEH and from 0.59 to 0.43 kcal/mol for the reaction of DMPBIH (Table 1). As compared to the change in ΔE_a from chloroform to acetonitrile, this change is smaller. We are not able to obtain the DAD_{PRC} information for the reactions in these solvents as it is not possible

to enter the specific solvent effects in computations, such as the H-bonding effect expected; but we determined the γ- and ε-CH_3/CD_3 2° KIEs on DMPBIH (0.89 (0.01)) and MA^+ (1.03 (0.01)) for their reaction in isopropanol/water to attempt to differentiate the DAD_{TRS} from that in acetonitrile (Tables S12 and S13). By comparison with the corresponding values in acetonitrile (0.88 and 1.03, Table 2), however, these 2° KIEs are not distinguishable within the experimental error (Table 2). This suggests that the DAD_{TRS}'s likely do not differ significantly in the two solvent systems. Therefore, we do not have direct DAD_{PRC}/DAD_{TRS} information to correlate with the ΔE_a's in between the protic *vs.* acetonitrile solvent systems. We regard that the protic solvent likely forms H-bonding with the reactant moieties of the TRS lengthening the DADs and lowering the TRS rigidity to a small extent so that only a slightly larger ΔE_a is observed.

On the other hand, a comparison of the ΔE_a's for the reactions of HEH *vs*. DMPBIH in Table 1 shows that the ΔE_a is significantly larger for the reaction of the less reactive HEH in all of the solvent systems. For example, they are 0.95 (HEH) *vs*. 0.43 (DMPBIH) in acetonitrile and 1.26 *vs.* 0.64 kcal/mol in chloroform. Since the HEH system (again, less reactive than the DMPBIH system) is able to sample more and longer DADs, this structural effects on ΔE_a also show that a more flexible system gives rise to a larger ΔE_a, which is consistent with our hypothesis as well.

▪ CONCLUSIONS

Effects of polar *vs.* less polar solvents and aprotic *vs.* protic solvents on the kinetics and T-dependence of KIEs (ΔE_a) of the two hydride transfer reactions from HEH and DMPBIH to MA^+ were carefully determined to investigate our hypothesis that a more rigid system gives rise to a smaller ΔE_a. The hydride-transfer takes place within the PRCs of CT complexations. The observed unusual ΔE_a's and 2° KIEs together with those from the analogous hydride transfer reactions from literature suggest that the class of reactions use a H-tunneling mechanism. The effects of selected aprotic solvents (acetonitrile *vs.* chloroform) on the DAD distributions were obtained by computations (for DAD_{PRC}) and from the analysis of the kinetic results including 2º KIEs (for DAD_{TRS}). Correlations between the ΔE_a's and DADs were presented.

We found, (1) both the average DAD_{PRC} and DAD_{TRS} are longer in chloroform than in acetonitrile; (2) the ΔE_a is larger in a less polar solvent (*e.g.*, chloroform > acetonitrile and isobutyronitrile > acetonitrile); (3) the ΔE_a is slightly larger in a protic (hydoxylic) solvent than an aprotic solvent of comparable polarity; and (4) the ΔE_a is larger for the reaction of less reactive HEH (*vs.* DMPBIH). Note that the solvent effects on the DADs are consistent with our expectations, which are, (a) a less polar solvent could destabilize the positively charged TRS loosening the CT complexation, *i.e.*, making a longer DAD_{TRS}; and (b) the system of more reactive DMPBIH (vs. HEH) forms a tighter TRS complex, *i.e.*, accompanying with a shorter DAD_{TRS}. No direct evidence shows a longer DAD in hydoxylic solvent than in aprotic solvent of acetonitrile, but the expected larger ΔE_a (although slightly) in the former solvent was observed. By comparison of the DAD information with the observed ΔE_a's, we draw a conclusion that the shorter and less broadly distributed DAD_{PRC}/DAD_{TRS}'s resulted from the stronger CT complexation vibrations give rise to a smaller ΔE_a. This supports our hypothesis.

Our work closely imitates the KIE studies of many hydride transfer reactions mediated by enzymes, especially the dihydrofolate reductases (DHFRs) for which the T-dependency of KIEs as well as the dynamical effects on catalysis have been extensively studied in literature.[8,25,31,34,35,41,44,77,83] Our reactions involve hydride transfer from the 1,4-dihydropyridine in HEH and the 1,2-dihydroimidazoline in DMPBIH to the $RN(CH_3)^+$=CH-CH=CHR' moiety in MA^+, whereas the reaction catalyzed by DHFR involves the hydride transfer from 1,4-dihydropyridine in NADPH to the RNH^+=CHR' moiety from the 5-N-protonated 7,8-dihydrofolate ($DHFH^+$) structure. Like many enzyme catalyzed H-

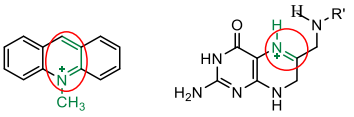

transfer reactions, wild-type DHFR gives rise to nearly T-independent KIEs ($\Delta E_{a(T-H)} \sim 0$, the subscript T is tritium) but the KIE becomes more and more T-dependent as the strategic site-directed mutagenesis to increase DADs were designed ($\Delta E_{a(T-H)}$ of as high as 3.31 kcal/mol[8]), or when its primitive forms that are believed to have a "destroyed" active site were used[25] (*e.g.*, $\Delta E_{a(T-H)}$ = 0.87 kcal/mol for the R67 DHFR[84] and 5.7 kcal/mol for the circularly permuted DHFR[25]). Indeed, our study of the T-dependent KIEs in acetonitrile *vs.* chloroform closely imitates the comparison study of the wild-type DHFR *vs.* the R67 DHFR. The latter primitive enzyme has a simpler (thinner) and looser protein structure, which results in a loose active site and even allows the environmental water to leak through making the KIE more T-dependent.[84,85] In our reaction, when the localized inner acetonitrile solvation shell around the TRS becomes thin enough to allow the chloroform to leak through, the CT-complexation in the TRS becomes loose and the KIE also becomes more T-dependent (insets **A** to **D** in Figure 4). The results from enzymes have been explained in terms of the destruction of the enzyme active site structure and thus the naturally evolved active site thermal vibrations so that the efficient short DAD_{TRS} sampling becomes difficult causing stronger T-dependence of KIEs. Our conclusion that the more rigid system gives rise to a smaller T-dependence of KIEs appears to support the explanation.

At last, we would like to emphasize that our results may also be simulated by other H-transfer/tunneling models to find other explanations and provide alternative insight into the protein functions in enzyme catalysis. At any rate, the results could be used to examine the existing H-tunneling models and could also be used to help build future potential hydride as well as general H-transfer/tunneling theories. Study of the effects of solvent viscosities on ΔE_a's for hydride transfer reactions to further understand the T-dependence of KIEs in enzymes and solution is currently in progress in this lab.

ASSOCIATED CONTENT

Supporting Information

The Arrhenius plots of 1° KIE's in various protic solvents, raw kinetic data, KIE/EIE computation procedures, as well as the atom coordinates, electronic energies, free energies of the computed ground-state reactants and products, classical TS's. This material is available free of charge via the Internet at http://pubs.acs.org.

AUTHOR INFORMATION

Corresponding Author

* yulu@siue.edu

Notes

The authors declare no competing financial interests.

ACKNOWLEDGMENT

Acknowledgment is made to the donors of the National Science Foundation (NSF# 1800194) for supporting of this research.

REFERENCES

(1) Cha, Y.; Murray, C. J.; Klinman, J. P. Hydrogen tunneling in enzyme reactions. *Science* **1989**, *243*, 1325-1330.

(2) Cleland, W. W.: Multiple isotope effects in enzyme-catalyzed reactions. In *Enzyme Mechanism from Isotope Effects*; Cook, P. F., Ed.; CRC Press: Boca Raton, Fl., 1991; pp 247-268.

(3) Nesheim, J. C.; Lipscomb, J. D. Large kinetic isotope effects in methane oxidation catalyzed by methane monooxygenase: Evidence for C-H bond cleavage in a reaction cycle intermediate. *Biochemistry* **1996**, *35*, 10240-10247.

(4) Hess, R. A.; Hengge, A. C.; Cleland, W. W. Isotope effects on enzyme-catalyzed acyl transfer from p-nitrophenyl acetate: concerted mechanisms and increased hyperconjugation in the transition state. *J. Am. Chem. Soc.* **1998**, *120*, 2703-2709.

(5) Nagel, Z. D.; Klinman, J. P. Update 1 of: Tunneling and dynamics in enzymatic hydride transfer. *Chem. Rev.* **2010**, *110*, PR41–PR67.

(6) Layfield, J. P.; Hammes-Schiffer, S. Hydrogen Tunneling in Enzymes and Biomimetic Models. *Chem. Rev.* **2014**, *114*, 3466–3494.

(7) Wang, Z.; Singh, P. N.; Czekster, M. C.; Kohen, A. S., V.L. Protein Mass-Modulated Effects in the Catalytic Mechanism of Dihydrofolate Reductase: Beyond Promoting Vibrations. *J. Am. Chem. Soc.* **2014**, *136*, 8333-8341.

(8) Stojkoviç, V., Perissinotti, L., Willmer, D., Benkovic, S., and Kohen, A. Effects of the donor acceptor distance and dynamics on hydride tunneling in the dihydrofolate reductase catalyzed reaction. *J. Am. Chem. Soc.* **2012**, *134*, 1738-1745.

(9) Bell, R. P.: *The tunnel effect in chemistry*; Chapman & Hall: London & New York., 1980.

(10) Kamerlin, S. C. L.; Warshel, A. An analysis of all the relevant facts and arguments indicates that enzyme catalysis does not involve large contributions from nuclear tunneling. *J. Phy. Org. Chem.* **2010**, *23*, 677-684.

(11) Truhlar, G. D. Tunneling in enzymatic and nonenzymatic hydrogen transfer reactions. *J. Phy. Org. Chem.* **2010**, *23*, 660-676.

(12) Schramm, V. L.; Schwartz, S. D. Promoting vibrations and the function of enzymes. Emerging theoretical and experimental convergence. *Biochemistry* **2018**, *57*, 3299-3308.

(13) Kohen, A. Role of Dynamics in Enzyme Catalysis: Substantial vs. Semantic Controversies. *Acc. Chem. Res.* **2015**, *48*, 466-473.

(14) Basran, J.; Sutcliffe, M. J.; Scrutton, N. S. Enzymatic H-Transfer Requires Vibration-Driven Extreme Tunneling. *Biochemistry* **1999**, *38*, 3218-3222.

(15) Kohen, A.; Cannio, R.; Bartolucci, S.; Klinman, J. P. Enzyme dynamics and hydrogen tunnelling in a thermophilic alcohol dehydrogenase. *Nature* **1999**, *399*, 496-499.

(16) Harris, R. J., Meskys, R., Sutcliffe, M. J., Scrutton, N. S. Kinetic Studies of the Mechanism of Carbon−Hydrogen Bond Breakage by the Heterotetrameric Sarcosine Oxidase of Arthrobacter sp. 1-IN. *Biochemistry* **2000** *39*, 1189-1198.

(17) Basran, J.; Sutcliffe, M. J.; Scrutton, N. S. Deuterium Isotope Effects during Carbon–Hydrogen Bond Cleavage by Trimethylamine Dehydrogenase: Implications for mechanism and vibrationally assisted hydrogen tunneling in wild-type and mutant enzymes. *J. Biol. Chem.* **2001**, *276*, 24581-24587.

(18) Knapp, M. J.; Klinman, J. P. Environmentally coupled hydrogen tunneling. Linking catalysis to dynamics. *Eur. J. Biochem.* **2002**, *269*, 3113–3121.

(19) Knapp, M. J.; Rickert, K.; Klinman, J. P. Temperature-dependent isotope effects in soybean lipoxygenase-1: Correlating hydrogen tunneling with protein dynamics. *J. Am. Chem. Soc.* **2002**, *124*, 3865-3874.

(20) Sikorski, R. S.; Wang, L.; Markham, K. A.; Rajagopalan, P. T. R.; Benkovic, S. J.; Kohen, A. Tunneling and coupled motion in the *E. coli* dihydrofolate reductase catalysis. *J. Am. Chem. Soc.* **2004**, *126*, 4778-4779.

(21) Wang, Z.; Kohen, A. Thymidylate synthase catalyzed H-transfers: Two chapters in one tale. *J. Am. Chem. Soc.* **2010**, *132*, 9820–9825.

(22) Hu, S.; Soudackov, A. V.; Hammes-Schiffer, S.; Klinman, J. P. Enhanced Rigidification within a Double Mutant of Soybean Lipoxygenase Provides Experimental Support for Vibronically Nonadiabatic Proton-Coupled Electron Transfer Models. *ACS Catal.* **2017**, *7*, 3569−3574.

(23) Li, P.; Soudackov, A. V.; Hammes-Schiffer, S. Fundamental insights into proton-coupled electron transfer in soybean lipoxygenase from quantum mechanical/molecular mechanics free energy simulations. *J. Am. Chem. Soc.* **2018**, *140*, 3068-3076.

(24) Howe, G. W.; van der Donk, W. A. Temperature-Independent Kinetic Isotope Effects as Evidence for a Marcus-like Model of Hydride Tunneling in Phosphite Dehydrogenase. *Biochemistry* **2019**, *58*, 4260-4268.

(25) Singh, P.; Vandemeulebroucke, A.; Li, J.; Schulenburg, C.; Fortunato, G.; Kohen, A.; Hilvert, D.; Cheatum, C. M. Evolution of the Chemical Step in Enzyme Catalysis. *ACS Catal.* **2021**, *11*, 6726–6732.

(26) Kuznetsov, A. M.; Ulstrup, J. Proton and hydrogen atom tunneling in hydrolytic and redox enzyme catalysis. *Can. J. Chem.* **1999**, *77*, 1085-1096.

(27) Pudney, C. R.; Johannissen, J. O.; Sutcliffe, M. J.; Hay, S.; Scrutton N. S. . Direct Analysis of Donor-Acceptor Distance and Relationship to Isotope Effects and the Force Constant for Barrier Compression in Enzymatic H-Tunneling Reactions. *J. Am. Chem. Soc.* **2010**, *132*, 11329-11335.

(28) Klinman, J. P.; Kohen, A. Hydrogen Tunneling Links Protein Dynamics to Enzyme Catalysis. *Annu. Rev. Biochem.* **2013**, *82*, 471–496.

(29) Hatcher, E.; Soudackov, A. V.; Hammes-Schiffer, S. Proton-coupled electron transfer in soybean lipoxygenase. *J. Am. Chem. Soc.* **2004**, *126*, 5763-5775.

(30) Salna, B.; Benabbas, A.; Russo, D.; Champion, P. M. Tunneling kinetics and nonadiabatic proton-coupled electron transfer in proteins: The effect of electric fields and anharmonic donor-acceptor interactions. *J. Phys. Chem. B* **2017**, *121*, 6869−6881.

(31) Pu, J.; Ma, S.; Gao, J.; Truhlar, D. G. Small temperature dependence of the kinetic isotope effect for the hydride transfer reaction catalyzed by Escherichia coli dihydrofolate reductase. *J. Phys. Chem. B* **2005**, *109*, 8551−8556.

(32) Kanaan, N.; Ferrer, S.; Martí, S.; Garcia-Viloca, M.; Kohen, A.; Moliner, V. Temperature Dependence of the Kinetic Isotope Effects in Thymidylate Synthase. A Theoretical Study. *J. Am. Chem. Soc.* **2011**, *133*, 6692–6702.

(33) Delgado, M. G., S.; Longbotham, J. E.; Scrutton, N. S.; Hay, S.; Moliner, V.; Tuñón, I. Convergence of Theory and Experiment on the Role of Preorganization, Quantum Tunneling, and Enzyme Motions into Flavoenzyme-Catalyzed Hydride Transfer. *ACS Catal.* **2017**, *7*, 3190–3198.

(34) Liu, H.; Warshel, A. Origin of the Temperature Dependence of Isotope Effects in Enzymatic Reactions: The Case of Dihydrofolate Reductase. *J. Phys. Chem. B* **2007**, *111*, 7852–7861.

(35) Agarwal, P. K.; Billeter, S. R.; Rajagopalan, P. T. R.; Benkovic, S. J.; Hammes-Schiffer, S. Network of coupled promoting motions in enzyme catalysis. *Proc. Natl. Acad. Sci. USA* **2002**, *99*, 2794–2799.

(36) Klinman, J. P. A new model for the origin of kinetic hydrogen isotope effects. *J. Phy. Org. Chem.* **2010**, *23*, 606–612.

(37) Klinman, J. P.; Offenbacher, A. R. Understanding Biological Hydrogen Transfer Through the Lens of Temperature Dependent Kinetic Isotope Effects. *Acc. Chem. Res.* **2018**, *51*, 1966–1974.

(38) Ludlow, M. K.; Soudackov, A. V.; Hammes-Schiffer, S. Theoretical Analysis of the Unusual Temperature Dependence of the Kinetic Isotope Effect in Quinol Oxidation. *J. Am. Chem. Soc.* **2009**, *131*, 7094–7102.

(39) Roston, D.; Cheatum, C. M.; Kohen, A. Hydrogen Donor-Acceptor Fluctuations from Kinetic Isotope Effects: A Phenomenological Model. *Biochemistry* **2012**, *51*, 6860-6870.

(40) Romero, E.; Ladani, S. T.; Hamelberg, D.; Gadda, G. Solvent-Slaved Motions in the Hydride Tunneling Reaction Catalyzed by Human Glycolate Oxidase. *ACS Catal.* **2016**, *6*, 2113−2120.

(41) Loveridge, E. J.; Tey, L.-H.; Allemann, R. K. Solvent Effects on Catalysis by Escherichia coli Dihydrofolate Reductase. *J Am Chem Soc* **2010**, *132*, 1137–1143.

(42) Pang, J.; Pu, J.; Gao, J.; Truhlar, D. G.; Allemann, R. K. Hydride Transfer Reaction Catalyzed by Hyperthermophilic Dihydrofolate Reductase Is Dominated by Quantum Mechanical Tunneling and Is Promoted by Both Inter- and Intramonomeric Correlated Motions. *J. Am. Chem. Soc.* **2006**, *128*, 8015-8023.

(43) Hatcher, E.; Soudackov, A. V.; Hammes-Schiffer, A. Proton-Coupled Electron Transfer in Soybean Lipoxygenase: Dynamical Behavior and Temperature Dependence of Kinetic Isotope Effects. *J. Am. Chem. Soc.* **2007**, *129*, 187–196.
(44) Fan, Y.; Cembran, A.; Ma, S.; Gao, J. Connecting Protein Conformational Dynamics with Catalytic Function As Illustrated in Dihydrofolate Reductase. *Biochemistry* **2013**, *52*, 2036-2049.
(45) Lu, Y.; Wilhelm, S.; Bai, M.; Maness, P.; Ma, L. Replication of the Enzymatic Temperature Dependency of the Primary Hydride Kinetic Isotope Effects in Solution: Caused by the Protein Controlled Rigidity of the Donor-Acceptor Centers? *Biochemistry* **2019**, *58*, 4035–4046.
(46) Maness, P.; Koirala, S.; Adhikari, P.; Salimraftar, N.; Lu, Y. Substituent Effects on Temperature Dependence of Kinetic Isotope Effects in Hydride-Transfer Reactions of NADH/NAD+ Analogues in Solution: Reaction Center Rigidity Is the Key. *Org. Lett.* **2020**, *22*, 5963–5967.
(47) Bai, M.; Koirala, S.; Lu, Y. Direct Correlation Between Donor-Acceptor Distance and Temperature Dependence of Kinetic Isotope Effects in Hydride-Tunneling Reactions of NADH/NAD+ Analogues. *J. Org. Chem.* **2021**, *86*, 7500–7507.
(48) Liu, Q.; Zhao, Y.; Hammann, B.; Eilers, J.; Lu, Y.; Kohen, A. A Model Reaction Assesses Contribution of H-Tunneling and Coupled Motions to Enzyme Catalysis. *J. Org. Chem.* **2012**, *77*, 6825–6833.
(49) Ma, L.; Sakhaee, N.; Jafari, S.; Wilhelm, S.; Rahmani, P.; Lu, Y. Imbalanced Transition States from α-H/D and Remote β-Type N-CH/D Secondary Kinetic Isotope Effects on the NADH/NAD+ Analogues in Their Hydride Tunneling Reactions in Solution. *J. Org. Chem.* **2019**, *84*, 5431–5439.
(50) Zhu, X. Q.; Deng, F. H.; Yang, J. D.; Li, X. T.; Chen, Q.; Lei, N. P.; Meng, F. K.; Zhao, X. P.; Han, S. H.; Hao, E. J.; et al. A classical but new kinetic equation for hydride transfer reactions. *Org. Biomol. Chem.* **2013**, *11*, 6071-6089.
(51) Shen, G. B.; Xia, K.; Li, X. T.; Li, J. L.; Fu, Y. H.; Yuan, L.; Zhu, X. Q. Prediction of Kinetic Isotope Effects for Various Hydride Transfer Reactions Using a New Kinetic Model. *J. Phys. Chem. A* **2016**, *120*, 1779−1799.
(52) Lee, I.-S. H.; Jeoung, E. H.; Kreevoy, M. M. Primary Kinetic Isotope Effects on Hydride Transfer from 1,3-Dimethyl-2-phenylbenzimidazoline to NAD+ Analogues. *J. Am. Chem. Soc.* **2001**, *123*, 7492-7496.
(53) Marenich, A. V.; Cramer, C. J.; Truhlar, D. G. Universal Solvation Model Based on Solute Electron Density and on a Continuum Model of the Solvent Defined by the Bulk Dielectric Constant and Atomic Surface Tensions. *J. Phys. Chem. B* **2009**, *113*, 6378–6396.
(54) Zhao, Y.; Truhlar, D. G. The M06 Suite of Density Functionals for Main Group Thermochemistry, Thermochemical Kinetics, Noncovalent Interactions, Excited States, and Transition Elements: Two New Functionals and Systematic Testing of Four M06-Class Functionals and 12 Other Functionals. *Theor. Chem. Acc* **2008**, *120*, 215–241.
(55) Weigend, F.; Ahlrichs, R. Balanced Basis Sets of Split Valence, Triple Zeta Valence and Quadruple Zeta Valence Quality for H to Rn: Design and Assessment of Accuracy. *Phys. Chem. Chem. Phys.* **2005**, *7*, 3297–3305.
(56) Alecu, I. M.; Zheng, J.; Zhao, Y.; Truhlar, D. G. Computational Thermochemistry: Scale Factor Databases and Scale Factors for Vibrational Frequencies Obtained from Electronic Model Chemistries. *J. Chem. Theory Comput.* **2010**, *6*, 2872–2887.
(57) Fukuzumi, S.; Ohkubo, K.; Tokuda, Y.; Suenobu, T. Hydride Transfer from 9-Substituted 10-Methyl-9,10-dihydroacridines to Hydride Acceptors via Charge-Transfer Complexes and Sequential Electron-Proton-Electron Transfer. A Negative Temperature Dependence of the Rates. *J. Am. Chem. Soc.* **2000**, *122*, 4286-4294.
(58) Lu, Y.; Zhao, Y.; Parker, V. D. Proton-transfer reactions of methylarene radical cations with pyridine bases under non-steady-state conditions. Real kinetic isotope effect evidence for extensive tunneling. *J Am. Chem. Soc.* **2001**, *123*, 5900-5907.
(59) Zhu, X. Q.; Zhang, J. Y.; Cheng, J.-P. Negative Kinetic Temperature Effect on the Hydride Transfer from NADH Analogue BNAH to the Radical Cation of N-Benzylphenothiazine in Acetonitrile". *J. Org. Chem.* **2006**, *71*, 7007-7015.
(60) Cook, P. F., Oppenheimer, N. J., Cleland, W. W. . Primary and secondary deuterium isotope effects on equilibrium constants for enzyme-catalyzed reactions. *Biochemistry* **1980**, *19*, 4853-4858.
(61) Cook, P. F.; Oppenheimer, N. J.; Cleland, W. W. Secondary deuterium and nitrogen- 15 isotope effects in enzyme-catalyzed reactions. Chemical mechanism of liver alcohol dehydrogenase. *Biochemistry* **1981**, *20*, 1817-1825.
(62) Lee, I.-S. H.; Jeoung, E. H.; Kreevoy, M. M. Marcus Theory of a Parallel Effect on R for Hydride Transfer Reaction between NAD+ Analogues. *J. Am. Chem. Soc.* **1997**, *119*, 2722-2728.
(63) Lu, Y.; Zhao, Y.; Handoo, K. L.; Parker, V. D. Hydride-exchange reactions between NADH and NAD+ model compounds under non-steady-state conditions. Apparent and Real kinetic isotope effects. *Org. Biomol. Chem.* **2003**, *1*, 173 - 181.
(64) Powell, M. F.; Bruice, T. C. Effect of isotope scrambling and tunneling on the kinetic and product isotope effects for reduced nicotinamide adenine dinucleotide model hydride transfer reactions. *J. Am. Chem. Soc.* **1983**, *105*, 7139–7149.
(65) Kil, H. J.; Lee, I.-S. H. Primary Kinetic Isotope Effects on Hydride Transfer from Heterocyclic Compounds to NAD + Analogues. *J. Phs. Chem. A* **2009**, *113*, 10704-10709.
(66) Kreevoy, M. M.; Ostovic, D.; Truhlar, D. G.; Garrett, B. C. Phenomenological manifestations of large-curvature tunneling in hydride-transfer reactions. *J. Phys. Chem.* **1986**, *90*, 3766-3774.
(67) Pagano, P.; Guo, Q.; Ranasinghe, C.; Schroeder, E.; Robben, K.; Häse, F.; Ye, H.; Wickersham, K.; Aspuru-Guzik, A.; Major, D. T.; et al. Oscillatory Active-Site Motions Correlate with Kinetic Isotope Effects in Formate Dehydrogenase. *ACS Catal.* **2019**, *9*, 11199−11206.
(68) Hammann, B.; Razzaghi, M.; Kashefolgheta, S.; Lu, Y. Imbalanced Tunneling Ready States in Alcohol Dehydrogenase Model Reactions: Rehybridization Lags behind H-Tunneling. *Chem Comm* **2012**, *48*, 11337-11339.
(69) Maharjan, B.; Raghibi Boroujeni, M.; Lefton, J.; White, O. R.; Razzaghi, M.; Hammann, B. A.; Derakhshani-Molayousefi, M.; Eilers, J. E.; Lu, Y. Steric Effects on the Primary Isotope Dependence of Secondary Kinetic Isotope Effects in Hydride Transfer Reactions in Solution: Caused by the Isotopically Different Tunneling Ready State Conformations? *J. Am. Chem. Soc.* **2015**, *137*, 6653 - 6661.
(70) Rucker, J.; Cha, Y.; Jonsson, T.; Grant, K. L.; Klinman, J. P. Role of internal thermodynamics in determining hydrogen tunneling in enzyme-catalyzed hydrogen transfer reactions. *Biochemistry* **1992**, *31*, 11489-11499.
(71) Bahnson, B. J.; Park, D. H.; Kim, K.; Plapp, B. V.; Klinman, J. P. Unmasking of hydrogen tunneling in the horse liver alcohol dehydrogenase reaction by site-directed mutagenesis. *Biochemistry* **1993**, *32*, 5503-5507.
(72) Bahnson, B. J.; Colby, T. D.; Chin, J. K.; Goldstein, B. M.; Klinman, J. P. A link between protein structure and enzyme catalyzed hydrogen tunneling. *Proc. Nat. Acad. Sci. U.S.A.* **1997**, *94*, 12797-12802.
(73) Rucker, J.; Klinman, J. P. Computational study of tunneling and coupled motion. *J. Am. Chem. Soc.* **1999**, *121*, 1997-2006.
(74) Alhambra, C.; Corchado, J. C.; Sanchez, M. L.; Gao, J.; Truhlar, D. G. Quantum dynamics of hydride transfer in enzyme catalysis. *J. Am. Chem. Soc.* **2000**, *122*, 8197-8203.
(75) Kohen, A.; Jensen, J. H. Boundary conditions for the Swain-Schaad relationship as a criterion for hydrogen tunneling. *J. Am. Chem. Soc.* **2002**, *124*, 3858-3864.
(76) Roston, D.; Kohen, A. A Critical Test of the "Tunneling and Coupled Motion" Concept in Enzymatic Alcohol Oxidation. *J. Am. Chem. Soc.* **2013**, *135*, 13624–13627.
(77) Stojković, V.; Kohen, A. Enzymatic H-transfer: Quantum tunneling and coupled motion from kinetic isotope effects. *Isr. J. Chem.* **2009**, *49*, 163-173.
(78) Horitani, M.; Offenbacher, A. R.; Carr, C. A. M.; Yu, T.; Hoeke, V.; Cutsail, G. E.; Hammes-Schiffer, S.; Klinman, J. P.; Hoffman, B. M. C-13 ENDOR Spectroscopy of Lipoxygenase-Substrate Complexes Reveals the Structural Basis for C-H Activation by Tunneling. *J. Am. Chem. Soc.* **2017**, *139*, 1984−1997.
(79) Ranasinghe, C.; Pagano, P.; Sapienza, P. J.; Lee, A. L.; Kohen, A.; Cheatum, C. M. Isotopic Labeling of Formate Dehydrogenase Perturbs the Protein Dynamics. *J. Phys. Chem. B* **2019**, *123*, 10403-10409.
(80) Perrin, C. L.; Ohta, B. K.; Kuperman, J.; Liberman, J.; Erdelyi, M. Stereochemistry of Beta-Deuterium Isotope Effects on Amine Basicity. *J. Am. Chem. Soc.* **2005**, *127*, 9641-9647.
(81) Perrin, C. L. The Logic behind a Physical−Organic Chemist's Research Topics. *J. Org. Chem.* **2017**, *82* 819−838.

(82) Driver, M. D.; Williamson, M. J.; Cook, J. L.; Hunter, C. A. Functional group interaction profiles: a general treatment of solvent effects on non-covalent interactions. *Chem. Sci.* **2020**, *11*, 4456-4466.
(83) Benkovic, S. J.; Hammes-Schiffer, S. A perspective on enzyme catalysis. *Science* **2003**, *301*, 1196-1202.
(84) Yahashiri, A.; Howell, E. E.; Kohen, A. Tuning of the H-Transfer Coordinate in Primitive versus Well-Evolved Enzymes. *Chem Phys Chem* **2008**, *9*, 980-982.
(85) Mhashal, A. R.; Major, D. T. Temperature-Dependent Kinetic Isotope Effects in R67 Dihydrofolate Reductase from Path-Integral Simulations. *J. Phys. Chem. B* **2021**, *125*, 1369–1377.

TOC Graphic

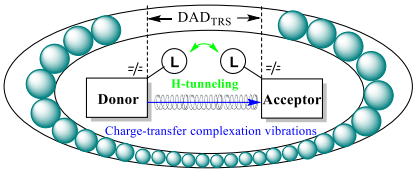

(L = H or D) **= Solvent molecule**

The stronger the solvation, the shorter the average DAD$_{TRS}$, the smaller the (E_{aD} - E_{aH})